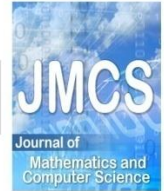Contents list available at JMCS

Journal of Mathematics and Computer Science

Journal Homepage: www.tjmcs.com

Robust Trajectory Tracking for a Flexible Probe in the Presence of Uncertainties and Disturbance

S. Zamiri[1], A. Vahidian Kamyad[2]

[1]Electrical Engineering Department, Gonabad Branch, Islamic Azad University, Gonabad, Iran
Zamiri.samira@yahoo.com
[2]Electrical Engineering Department, Ferdowsi University of Mashhad. Mashhad, Iran
Kamyad@math.um.ac.ir

Abstract

This paper investigates the trajectory tracking of a bio-inspired flexible probe in medical where there exist of uncertainty and disturbance in the system. In the first approach, a sliding mode controller is designed to deal with the uncertainties and output disturbances in the system. In this case, it is assumed that the upper band of uncertainty in the system is known, but in practice this may not be really possible. Therefore, in the next section, the sliding mode controller has been extended to a robust – adaptive controller in such a way that even if there is no information on the uncertainty upper bond, the system is still stable and the probe continues to track the desired trajectory. In this case, an adaptive rule has been designed to estimate the upper bound of the uncertainty and disturbance. A numerical simulation shows the effectiveness of the proposed methodologies.

Keywords: Bio-inspired flexible probe, Sliding mode control, Robust-adaptive control.

1. Introduction

Among a lot of techniques that are available for the surgeon, percutaneous intervention has attracted great interest, because it is performed through a very small port through the soft tissue, i.e., skin [1]. Entering into the body tissues through the skin and by probes and needles develops far fewer risks than open surgery for patients and thus is a treatment of choice in many clinical applications [2-3]. Needle insertion into soft tissue has many clinical applications such as tissue biopsy [4], brachytherapy [5], and anesthetic delivery [6]. When a path in to the tissue does not seem possible or is not safe, a flexible probe or needle can be utilized instead of a rigid probe to reach the target while avoiding special areas or obstacle avoidance. On the other hand, using flexible probe impose less pain to the patient.

Different models have been provided for bevel-tip flexible probe which predict needle-tip deviations from the target for compensation. Webster et al. proposed a kinematic model for probe deflections by generalizing the standard nonholonomic unicycle and bicycle models [7].

Due to the lack of an accurate on dynamic model of needle-tissue systems [8], most of the related studies are on computer simulations [9-10], pre-planning [11], steering [12] and path-planning [13], rather than the automatic control of the flexible needle. Path-planning, by itself, is not sufficient to proceed to robot-assisted needle insertion, unless there is a control system which can control the needle to track the designed path. Pre-planning is an offline process in which the needle insertion parameters such as the insertion angle and bevel orientation are derived prior to the insertion [11]. Steering is a closer approach to a control strategy. DiMaio et al. [12] derived a needle manipulation Jacobian, which relates the desired needle tip to base velocities, using a numerical needle insertion model that includes needle deflection and tissue deformation. Glozman et al. [14] used the analytical forward and inverse kinematics of a simplified needle-tissue model to determine the required needle base trajectory for any desired needle tip trajectory. Contrary to other approaches, we are currently developing a bio-inspired flexible probe [15-16], which can change its direction smoothly by means of a programmable bevel tip.

Robot-assisted needle insertion has recently received significant attention because of its potential capability in delivering accurate targeting [17], [18], [19], [20]. Due to the lack of an accurate model for the coupled needle-tissue system [21], most of the related studies are focused on computer simulations [22], [23], pre-planning [24], steering [25], and path-planning [26], rather than the automatic control of the flexible needle.

Closed loop control of the probe tip along an arbitrary smooth trajectory can be achieved without the need for an external imaging system. The authors in [27-28] have been showed that the concept of a programmable bevel tip is viable through experiments with a first 12 mm outer diameter prototype, where two-dimensional trajectory following can be achieved by means of a state feedback controller employing approximated linearization and a chained form representation. Webster et al. first proposed a kinematic model of the beveled tip needle to describe its behavior in soft tissue [29]. Alterovitz et al. then derived a motion-planning algorithm under uncertainty to obtain better targeting accuracy [30].

As the needle is inserted, asymmetric tissue forces cause the tip to deflect and follow a curved path through the tissue, which the flexible shaft follows. Asymmetric tip designs can be passive (e.g., using a beveled, prebent (kinked), precurved, or flexure tip) [31], [32] or actuatable [33], [34].

Reed et al. modeled the torsional dynamics of a flexible needle to analyze torsional behavior during needle insertion [35]. These studies have predominantly focused on open-loop trajectory following. Glozman and Shoham closed the control loop in their original approach [36] by means of fluoroscopic images, which were used to measure needle deflection during the insertion process [37]. Recently, [38] designed a model predictive controller for a bio-inspired flexible probe to track a desired trajectory. On the other hand, for generating multiple trajectories with a fixed bevel tip, Minhas et al. [39, 40] and Wood et al. [41] proposed a duty-cycling spinning algorithm – by periodically changing the orientation of the needle along its long axis by means of a base-mounted revolute actuator, trajectories with different radii could be achieved. Specifically, [42] utilized fluoroscopic images to measure the deflection of a stiff needle (without bevel tip) when inserted into tissue.

In previous studies on bio-inspired flexible probes, it has been assumed that the model of probe is exact and there is no disturbance and uncertainty in the system. Actually, according to the movement of the probe tip into the tissue and the lack of detailed knowledge of the tissue, the model is subject to the noise and disturbance. This unknown disturbance may accrue because of the vessels and the unpredictable movement of tissues in the direction of the probe path. In this case, a term as disturbance and noise must be added to the kinematic model of probe.

In this paper, the problem of trajectory tracking of a bio-inspired flexible probe with consideration of uncertainty and disturbance in the system model has been studied. With assumption that the upper band of uncertainty in the system is known a sliding mode controller is designed to deal with the

uncertainties and output disturbances in the system. In practice, knowing the upper bound of disturbances may not be really possible. Therefore, the sliding mode controller has been extended to a robust-adaptive controller in such a way that, even if there is no information on the uncertainty upper bond, the probe continues to track the desired trajectory.

This paper is organized as follows: The problem formulation and some preliminaries are given in Section II. Section III presents the main results of this paper that is designing the tracking controller for the probe in presence of uncertainty and disturbance. A robust sliding mode controller and a robust- adaptive controller have been designed in this Section. Simulation results in Section IV are given to confirm the analytical results. Finally, conclusions in Section V close the paper.

2. Problem formulation

The kinematic model of a bio-inspired flexible probe can be expressed by the following nonlinear model [24]:

$$
\begin{bmatrix} \dot{x} \\ \dot{y} \\ \dot{\theta} \\ \dot{\delta} \end{bmatrix} = \begin{bmatrix} cos\theta \\ sin\theta \\ k(\delta - \varepsilon\theta) \\ 0 \end{bmatrix} u_1 + \begin{bmatrix} 0 \\ 0 \\ 0 \\ 1 \end{bmatrix} u_2 \tag{1}
$$

where δ indicates the steering offset, k indicates a coefficient between the steering offset and the curvature of the probe, ε indicates the compensation coefficient caused by the shape of the probe, θ indicates the tip angle of the probe and u_1 and u_2 respectively denote the linear velocity and the rate of change of steering offset of the probe (Fig. 1)

(a)
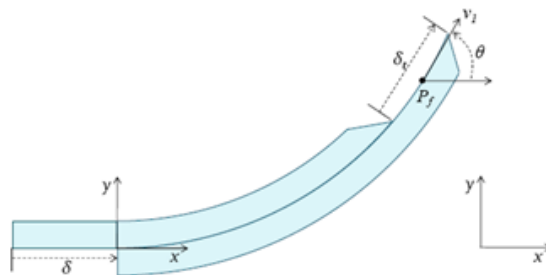
(b)

Fig. 1 The bio-inspired flexible probe. The probe that is following a trajectory [24]. The model of a Flexible probe

Actually, the bevel tip of probe is controlled by applying a force to the base of the probe and probe's motion is due to the relative position between two segments of the probe so-called steering offset [18]. The aim of the probe control is leading to an optimal point in the tissue of the body. To reach this point, an optimal path is determined to deal with possible obstacles or damaging to the body tissues.

Defining $q = [x, y, \theta, \delta]$ as the generalized coordinates of the probe and $u = [u_1, u_2]^T$ as input velocities, the model in (1) can be written as

$$\dot{q} = G(q)u \tag{2}$$

Where

$$G(q) = \begin{bmatrix} \cos\theta & 0 \\ \sin\theta & 0 \\ k(\delta - \varepsilon\theta) & 0 \\ 0 & 1 \end{bmatrix} \tag{3}$$

The model introduced in (2) does not express the exact behavior of the probe. For example, the relation between instantaneous curvature (ρ) and the steering offset in the tip of probe (δ_t) has been considered with a linear function with the coefficient k (mm^{-2})[24].This relation may be more complicated and with this assumption, some parts of the motion behavior of probe may be ignored. So, in the following model, we have considered such modeling uncertainties

$$\dot{q} = (G(q) + \Delta G(q))u \tag{4}$$

Where $\Delta G(q)$ denotes the additive uncertainty in the kinematic model introduced in (2).

In addition, according to the movement of the probe tip into the tissue and the lack of detailed knowledge of the tissue, the model in (2) is subject to the noise and disturbance. This unknown disturbance may accrue because of the vessels and the unpredictable movement of tissues in the direction of the probe path. In this case, a term as disturbance and noise must be added to the kinematic model in (2). In fact, considering the effects of noise and disturbance, more accurately describes the behavior of the probe. So, rewrite the model in (2) as

$$\dot{q} = G(q)u + E(t) \tag{5}$$

Where $E(t) = [E_1(t), E_2(t), E_3(t), E_4(t)]^T$ denotes the disturbance and noise in the probe model that there is no information about them, unless we assume that this disturbance is bounded and we know the upper bound of it i.e.

$$\left| E_i(t) \right| \leq \alpha_i, i = 1, \ldots, 4 \tag{6}$$

where α_i $i = 1, \ldots, 4$ indicate the upper bound of disturbance and noise.

Considering both uncertainty and disturbance in the kinematic model of probe, one can easily combine the two models in (4) and (5) as follow

$$\dot{q} = G(q)u + d(t)$$
$$d(t) = \Delta G(q)u + E(t) \tag{7}$$

In this model $d(t) = [d_1(t), d_2(t), d_3(t), d_4(t)]^T$ describes both the model uncertainty and disturbance in the system. It is assumed that we only know the upper bound of the elements of $d(t)$ as follows

$$\left| d_i(t) \right| \le \varepsilon_i, i = 1, \ldots, 4 \tag{8}$$

Where $\varepsilon_i \in R^+$ denotes the upper bound of the summation of the disturbance and uncertainty in (7). Now, according to the (2) and (7), the equation of each state variable can be written as follow

$$\dot{x} = \cos\cos(\theta)u_1 + d_1 \qquad \left| d_1(t) \right| \le \varepsilon_1 \tag{9}$$

$$\dot{y} = \sin\sin(\theta)u_1 + d_2 \qquad \left| d_2(t) \right| \le \varepsilon_2 \tag{10}$$

$$\dot{\theta} = k(\delta - \varepsilon\theta)u_1 + d_3 \left| d_3(t) \right| \le \varepsilon_3 \tag{11}$$

$$\dot{\delta} = u_2 + d_4 \left| d_4(t) \right| \le \varepsilon_4 \tag{12}$$

3. Design of tracking controller

The aim of this Section is to design a controller for the flexible probe that is described in (9-12), to track a desired trajectory. Note that the rank of the matrix $G(q)$ in (3) around any equilibrium point is two. This means that only two state variable of the probe in the model can be controlled to reach a desired point or track a desired trajectory. In this Section, a sliding mode controller has been designed in such a way that the position of the probe tip e.g. $[x, y]^T$ tracks a desired trajectory $[x_{des}, y_{des}]^T$.

In the part A of this Section, a sliding mode controller is designed for the system in (9-12) to deal with the uncertainties and disturbances. In this case, it is assumed that the upper band of uncertainty in the system is known, but we know that in practice, this may not be really possible. Therefore, in part B, a robust – adaptive controller has been designed in such a way that, even if there is no information on the uncertainty upper bond, the system is still stable and the probe continues to track the desired trajectory.

A. Robust sliding mode controller

The sliding mode controller has been designed using back stepping in the following three steps:

Step 1: design u_1 and θ in (9) and (10) in such a way that $[x, y]^T$ tracks $[x_{des}, y_{des}]^T$.

Step 2: design δ in (11) in such a way that θ converges to θ that is designed in the previous step (θ_{des}).

Step 3: design u_2 in (12) in such a way that δ converges to δ that is designed in the previous step (δ_{des}).

Step 1: Design u_1 and θ

First, consider the following change of variables

$$v_1 = \cos\cos(\theta)u_1 \tag{13}$$

$$v_2 = \sin\sin(\theta)u_1$$

So, the equations in (9) and (10) can be written as

$$\dot{x} = v_1 + d_1$$
$$\dot{y} = v_2 + d_2$$
(14)

Now, the problem is finding v_1 and v_2 in presence of unknown uncertainties d_1 and d_2 such that x and y converge to the x_{des} and y_{des} respectively. The controller design has been presented for the first equation in (14) and designing controller for the second equation in (14) is quite similar.

Considering the error as $\tilde{x} = x - x_{des}$, we choose the integral sliding surface s(t) as below

$$s(t) = \tilde{x} + \int_0^t \Lambda \tilde{x}(\tau) d\tau$$
(15)

Where $s(t) \in \mathbb{R}$ and $\Lambda > 0$ is an arbitrary positive constant.

To establish the sliding mode, the reaching condition has been selected as

$$\dot{s}(t) = -rs - \rho sgn(s)$$
(16)

Where r and ρ are positive constants.

We select the input control v_1 as follow for the system in (14)

$$v_1 = \dot{x}_{des} - \Lambda \tilde{x} - rs - \rho sgn(s)$$
(17)

Substituting (17) into (14) results in the following equation for the closed loop system

$$\dot{s}(t) = -rs - \rho sgn(s) + d_1$$
(18)

It is shown in the following theorem that the input control (17) will stabilize the system in (14) if $\rho > \varepsilon_1$. This means that we should know the upper bound of d_1.

Theorem1. Consider the first equation in (14). By applying the input control (17) with $\Lambda > 0, r > 0$ and $\rho > \varepsilon_1$, the closed loop system of error is asymptotically stable and x exponentially converges to x_{des}. In this case, ε_1 denotes the upper bound of the uncertainty and disturbance denoted by d_1.

Proof: Consider the following Lyapunov candidate function:

$$V = \frac{1}{2}s^2$$
(19)

Taking the derivative of V with respect to time and substituting from (14), (15) and (17) results in

(20)

$$\dot{V} = s\dot{s} = s(\dot{\tilde{x}} + \Lambda\tilde{x}) = s(\dot{x} - \dot{x}_{des} + \Lambda\tilde{x}) = s(v_1 + d_1 - \dot{x}_{des} + \Lambda\tilde{x}) = s(\dot{x}_{des} - \Lambda\tilde{x} - rs - \rho sgn(s) + d_1 - \dot{x}_{des} + \Lambda\tilde{x}) = s(-rs - \rho sgn(s) + d_1)$$

$$= s(-rs - \rho sgn(s) + d_1) = -r|s|^2 - \rho|s| + sd_1 \leq -r|s|^2 - \rho|s| + |s||d_1| \leq -r|s|^2 + (\varepsilon_1 - \rho)|s|$$

Equation (20) shows that the condition $\rho > \varepsilon_1$ is a sufficient condition for the derivative of lyapunov function to be negative.

Using Lyapunov theorems, negativity of the derivative of Lyapunov function shows that s(t) and ṡ(t)tends to zero. So

$$\dot{s}(t) = \dot{\tilde{x}} + \Lambda\tilde{x} = 0 \Rightarrow \dot{\tilde{x}} = -\Lambda\tilde{x} \tag{21}$$

And this means that

$$\dot{\tilde{x}} = -\Lambda\tilde{x} \Rightarrow \tilde{x} = e^{-\Lambda t}\tilde{x}(0) \Rightarrow \tilde{x} \to 0 \Rightarrow x \to x_{des} \tag{22}$$

Design of the input controller v_2 for the second equation in (14) is similar to (17). So, without loss of generality we can consider both v_1 and v_2 as follow

$$v_1 = \dot{x}_{des} - \Lambda_1\tilde{x} - r_1 s_1 - \rho_1 \operatorname{sgn}(s_1)$$

$$v_2 = \dot{y}_{des} - \Lambda_2\tilde{y} - r_2 s_2 - \rho_2 \operatorname{sgn}(s_2) \tag{23}$$

Where $\Lambda_1, \Lambda_2, r_1, r_2$ are real positive constants and the inequalities $\rho_1 > \varepsilon_1$ and $\rho_2 > \varepsilon_2$ should be satisfied. On the other hand, the sliding surfaces s_1 and $s_2$are defined as follow

$$s_1(t) = \tilde{x} + \int_0^t \Lambda_1\tilde{x}(\tau)d\tau$$

$$s_2(t) = \tilde{y} + \int_0^t \Lambda_2\tilde{y}(\tau)d\tau \tag{24}$$

Now, after achieving v_1 and v_2 from (23), according to the equations in (13)u_1 and the desired θ (θ_{des}) can be obtained from the following relations

$$u_1 = \sqrt{v_1^2 + v_2^2}$$

$$\theta_{des} = \tan^{-1}\left(\frac{v_2}{v_1}\right) \tag{25}$$

Assumption 1: It is assumed in this paper that$u_1 \neq 0$.

This assumption means that during achieving the desired point, the probe must not be stopped.

Step 2: Design δ

In this step, the steering offset δ in (11) has been designed in such a way that θ converges to θ_{des} in (25).

Consider the equation in (11) as follows

$$\dot{\theta} = k\left(\delta - \varepsilon\theta\right)u_1 = A\theta + B\delta + d_3 \tag{26}$$

Where $A \triangleq -k\varepsilon u_1$ and $B \triangleq ku_1$. Define a new sliding surface as follows

$$s_3(t) = \tilde{\theta} + \int_0^t \Lambda_3 \tilde{\theta}(\tau)d\tau \tag{27}$$

where $\tilde{\theta} = \theta - \theta_{des}$ and Λ_3 is a arbitrary positive constant. Now, choosing δ as below for the system in (26) results in $\theta \to \theta_{des}$

$$\delta_{des} = \frac{1}{B}\left\{\dot{\theta}_{des} - \Lambda_3\tilde{\theta} - A\theta - r_3 s_3 - \rho_3 \operatorname{sgn}(s_3)\right\} \tag{28}$$

Where r_3, Λ_3 and ρ_3 are positive constants. It should be noted that according to the Assumption 1, $B \neq 0$ and we can use $1/B$ in (26).

Theorem2. Consider the equation in (11). By applying the input steering offset δ as in (28) with $\Lambda_3 > 0, r_3 > 0$ and $\rho_3 > \varepsilon_3$, the closed loop system of error is asymptotically stable and θ exponentially converges to θ_{des}. In this case ε_3 denotes the upper bound of the uncertainty and disturbanced_3.

Proof: consider the following lyapunov candidate function:

$$V = \frac{1}{2}s_3^2 \tag{29}$$

Taking the derivative of V with respect to time results in

$$
\begin{aligned}
\dot{V} = s_3\dot{s}_3 &= s_3\left(\dot{\tilde{\theta}} + \Lambda_3\tilde{\theta}\right) = s_3\left(\dot{\theta} - \dot{\theta}_{des} + \Lambda_3\tilde{\theta}\right) = s_3\left(A\theta + B\delta + d_3 - \dot{\theta}_{des} + \Lambda_3\tilde{\theta}\right) \\
&= s_3\left(A\theta + B\frac{1}{B}\{\dot{\theta}_{des} - \Lambda_3\tilde{\theta} - A\theta - r_3 s_3 - \rho_3 sgn(s_3)\} + d_3 - \dot{\theta}_{des} + \Lambda_3\tilde{\theta}\right) \\
&= s_3(-r_3 s - \rho_3 sgn(s_3) + d_3) = -r_3|s_3|^2 - \rho_3|s_3| + s_3 d_3 \\
&\leq -r_3|s_3|^2 - \rho_3|s_3| + |s_3||d_3| \leq -r_3|s_3|^2 + (\varepsilon_3 - \rho_3)|s_3|
\end{aligned}
\tag{30}
$$

Equation (30) shows that the condition$\rho_3 > \varepsilon_3$ is a sufficient condition for the negativity of derivative of lyapunov function.

Similar to the Theorem 1 and using lyapunov conditions, negativity of the derivative of lyapunov function results in convergence of θ to θ_{des}.

$\square$

Step 3: Design u_2

The last step of designing the tracking controller is to design u_2 in (12) such thatδ converges to the δ_{des} in (28). This u_2 has been offered as below

$$u_2 = \dot{\delta}_{des} - \Lambda_4\tilde{\delta} - r_4 s_4 - \rho_4 \operatorname{sgn}(s_4) \tag{31}$$

Where

$$s_3(t) = \tilde{\delta} + \int_0^t \Lambda_4 \tilde{\delta}(\tau) d\tau \quad \Lambda_4 > 0 \quad r_4 > 0 \quad \rho_4 > \varepsilon_4 \tag{32}$$

Theorem3. Consider the equation in (12). By applying u_2 as (31) with$\Lambda_4 > 0$, $r_4 > 0$ and$\rho_4 > \varepsilon_4$, the closed loop system is asymptotically stable and δ exponentially converges to δ_{des}. In this case ε_4 denotes the upper bound of the uncertainty and disturbanced_4.

Proof. The proof is similar to the proof of theorems 1 and 2.

By designing u_1 and u_2 from Theorems 1 and 3 respectively, the probe tip tracks the desired path $[x_{des}, y_{des}]^T$ in the presence of uncertainty and disturbance$d(t)$.

B. Robust-Adaptive controller

In the previous part, it has been assumed that the upper band of uncertainties in the system e.i. ε_i, $i = 1, \dots, 4$ are known and available, while it may not be possible in practice. Therefore, in this part, the previous controllers have been extended and for each equation, a robust- adaptive controller has been designed in such a way that the system tracks the desired trajectory even if there is no information of the upper band of uncertainty and disturbance in the system. For each case, a sliding mode control has been used and an adaptive law has been designed to estimate the upper bound of the uncertainty.

Similar to the part A, the robust-adaptive tracking controller is designed in three steps:

Step 1: Design u_1 and θ

Consider the first equation in (14) and suppose that $\bar{\varepsilon}_1$ is an estimation of the upper bound of$d_1(\varepsilon_1)$. Now, instead of (17), consider the input control v_1 as follows

$$v_1 = \dot{x}_{des} - \Lambda \tilde{x} - rs - \rho \bar{\varepsilon}_1 \, \text{sgn}(s) \tag{33}$$

Where the parameter $\bar{\varepsilon}_1$ is obtained from the following adaptive update law

$$\dot{\bar{\varepsilon}}_1 = K \rho s \, \text{sgn}(s) \tag{34}$$

Where $K > 0$ is adaptive gain? Actually $\bar{\varepsilon}_1$ that is an estimation of upper bound of uncertainty and disturbance, is estimated from the equation in (34). Now, consider the following Theorem.

Theorem4. Consider the first equation in (14). By applying the input control (33) with$\Lambda > 0$, $r > 0$ and $\rho > 1$ along with the adaptive law in (34) with$K > 0$, the closed loop system of error is asymptotically stable and x exponentially converges to x_{des}.

Proof: Consider the following lyapunov candidate function:

$$V = \frac{1}{2} s^2 + \frac{1}{2k} \tilde{\varepsilon}_1(t)^2 \tag{35}$$

Where $\tilde{\varepsilon}_1(t) = \bar{\varepsilon}_1(t) - \varepsilon_1$. Taking the derivative of V with respect to time and substituting from (33) and (34) results in

$$\dot{V} = s\dot{s} + \frac{1}{k}\bar{\varepsilon}_1\dot{\bar{\varepsilon}}_1 = s(-rs - \rho\bar{\varepsilon}_1 sgn(s) + d_1) + \frac{1}{k}\bar{\varepsilon}_1\dot{\bar{\varepsilon}}_1$$

$$= -r|s|^2 - \rho\bar{\varepsilon}_1 s sgn(s) + sd_1 + \frac{1}{k}\bar{\varepsilon}_1 k\rho s\, sgn(s) \tag{36}$$

$$= -r|s|^2 - \rho\bar{\varepsilon}_1 s sgn(s) + sd_1 + (\bar{\varepsilon}_1 - \varepsilon_1)\rho s\, sgn(s)$$

$$\le -r|s|^2 - \varepsilon_1\rho s\, sgn(s) + |s|\varepsilon_1 \le -r|s|^2 + (1-\rho)\varepsilon_1|s| < 0$$

Equation (36) shows that the condition $\rho > 1$is a sufficient condition for the derivative of lyapunov function to be negative. Similar to the Theorem 1, negativity of the derivative of lyapunov function results in convergence of x tox_{des}.

As it is clear, design of the input controller v_2 for the second equation in (14) is similar to (33). So, without loss of generality we can consider both v_1 and v_2 as follow

For the first equation in (14) we have

$$v_1 = \dot{x}_{des} - \Lambda_1\tilde{x} - r_1 s_1 - \rho_1\bar{\varepsilon}_1 sgn(s_1)$$
$$\dot{\bar{\varepsilon}}_1 = K_1\rho_1 s_1\, sgn(s_1) \tag{37}$$

And for the second equation we have

$$v_2 = \dot{y}_{des} - \Lambda_2\tilde{y} - r_2 s_2 - \rho_2\bar{\varepsilon}_2 sgn(s_2)$$
$$\dot{\bar{\varepsilon}}_2 = K_2\rho_2 s_2\, sgn(s_2) \tag{38}$$

Where $\Lambda_1, \Lambda_2, r_1, r_2, K_1$ and K_2 are real positive constants and the conditions $\rho_1 > 1$and $\rho_2 > 1$ are satisfied. After designing $v_1$and v_2, u_1 and θ_{des} can be obtained from the equation in (25).

Step 2: Design δ

The steering offset δ in (11) has been designed in this step, in such a way that even if there is no information ond_3, θ converges to θ_{des}(θ_{des} is obtained from the previous step)

Consider the equations in (26) and (27), chooseδ as below for the system in (26)

$$\delta_{des} = \frac{1}{B}\{\dot{\theta}_{des} - \Lambda_3\tilde{\theta} - A\theta - r_3 s_3 - \rho_3\bar{\varepsilon}_3 sgn(s_3)\} \tag{39}$$

Where r_3, Λ_3 and ρ_3 are positive constants and $\bar{\varepsilon}_3$ is obtained from the following adaptive law

$$\dot{\bar{\varepsilon}}_3 = K_3\rho_3 s_3\, sgn(s_3) \tag{40}$$

Where $K_3 > 0$ is the adaptive gain?

Theorem5. Consider the equation in (11). By applying the input steering offset δ as (39) with $\Lambda_3 > 0$, $r_3 > 0$ and $\rho_3 > 1$ along with the adaptive law in (40) with $K_3 > 0$,θ exponentially converges to θ_{des} . In this case $\bar{\varepsilon}_3$ denotes the estimation of the upper bound of the uncertainty and disturbanced_3.

Proof: consider the following lyapunov candidate function:

$$V = \frac{1}{2}s_3{}^2 + \frac{1}{2k_3}\tilde{\varepsilon}_3(t)^2 \tag{41}$$

Taking the derivative of V with respect to time results in

$$\dot{V} = s_3 \dot{s}_3 + \frac{1}{k_3} \tilde{\varepsilon}_3 \dot{\tilde{\varepsilon}}_3 = s_3(-r_3 s_3 - \rho_3 \bar{\varepsilon}_3 sgn(s_3) + d_3) + \frac{1}{k_3} \tilde{\varepsilon}_3 \dot{\tilde{\varepsilon}}_3$$

$$= -r_3 |s_3|^2 - \rho_3 \bar{\varepsilon}_3 s_3 sgn(s_3) + s_3 d_3 + (\bar{\varepsilon}_3 - \varepsilon_3) \rho_3 s_3 sgn(s_3)$$

$$\leq -r_3 |s_3|^2 - \varepsilon_3 \rho_3 s_3 sgn(s_3) + \varepsilon_3 |s_3| \leq -r_3 |s_3|^2 + (1 - \rho_3) \varepsilon_3 |s_3| < 0$$

(42)

Equation (42) shows that the condition $\rho_3 > 1$ is a sufficient condition for the negativity of derivative of lyapunov function.

Similar to the Theorem 4 and using lyapunov conditions, negativity of the derivative of lyapunov function results in convergence of θ to θ_{des}.

$\square$

Step 3: Design u$_2$

The last step of designing the tracking controller is to design u_2 in (12) such that δ converge to the δ_{des} in (39). This u_2 has been offered as below

$$u_2 = \dot{\delta}_{des} - \Lambda_4 \tilde{\delta} - r_4 s_4 - \rho_4 \bar{\varepsilon}_4 sgn(s_4)$$

(43)

Where $\bar{\varepsilon}_4$ is an estimation of ε_4 and is obtained from the following equation

$$\dot{\bar{\varepsilon}}_4 = K_4 \rho_4 s_4 \, sgn(s_4), \quad K_4 > 0$$

(44)

Theorem6. Consider the equation in (12). By applying u_2 in (43) with $\Lambda_4 > 0$, $r_4 > 0$ and $\rho_4 > 1$, the closed loop system of error is asymptotically stable and δ exponentially converges to δ_{des} . In this case $\bar{\varepsilon}_4$ denotes the estimation of the upper bound of the uncertainty and disturbance d_4.

Proof. The proof is similar to the proof of Theorems4 and 5.

By designing u_1 and u_2 from Theorems 4 and 6 respectively, the probe tip tracks the desired path $[x_{des}, y_{des}]^T$ in the presence of uncertainty and disturbance $d(t)$ and when there is no information on $d(t)$.

4. Numerical simulations

Some numerical examples have been presented in this Section to clarify the results of the previous section

Example 1: Consider the following desired path for the flexible probe

$$x_{des} = t$$

$$y_{des} = \sin\left(\frac{t}{2}\right)$$

(45)

Suppose the uncertainty and disturbance $d_i(t), i = 1,2, \dots ,4$ for all equations in (9)-(12) is a random number between 1 and 2. So, an upper bound for $d_i(t)$ can be considered as ($\varepsilon_1 = \varepsilon_2 = \varepsilon_3 = \varepsilon_4 = 2$). The aim is to design an robust sliding mode controller using theorems 1- 4. To use this theorem we choose $\rho = 3$ for all of them that is larger than the upper bound of uncertainties. The other controller parameters have been chosen as follow (they have been considered same for all of sliding mode controllers)

$$\Lambda = 5, \qquad r = 3$$

(46)

On the other hand, the probe parameters have been considered as [24]

$$\varepsilon = 7.2, \quad k = 0.28$$

(47)

Considering the initial condition of probe as $[x_0, y_0]^T = [1, -2]^T$, the results of simulation have been shown in Fig. 1 and Fig. 2. The tracking errors have been shown in Fig. 1. This figure confirms that errors converge to zero. It is worth mention that some oscillations in the error signals that called

chattering, are because of the function sgn(s) in the input controllers. To counteract this phenomenon, there are some ways for example adding a damped continues term along with the sgn(s) with the aim of continuous improvement of control signal.
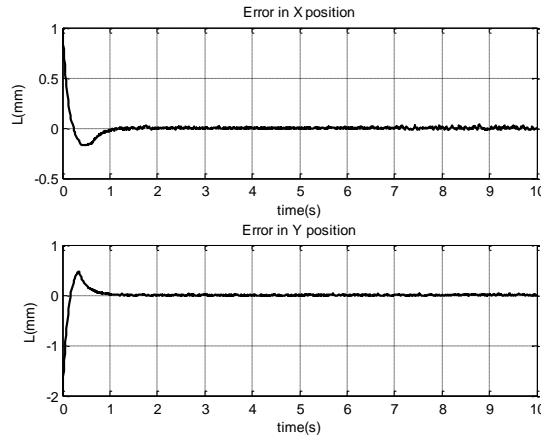

Fig 2. Tracking errors in the direction of x and y in Example 1

Fig. 2 shows the trajectory of probe along with the desired trajectory. This Figure confirms that in the presence of uncertainty and disturbances, the probe tracks the desired trajectory well.
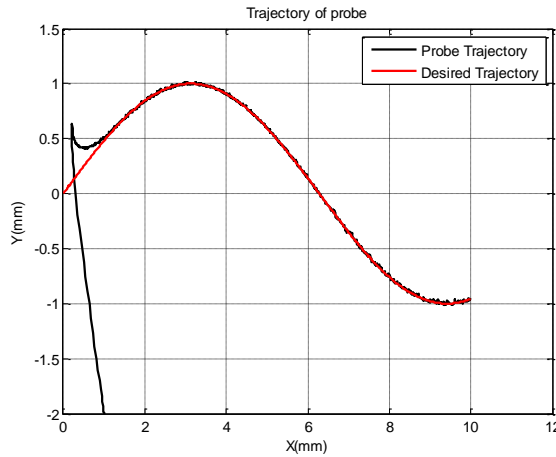

Fig 3. Probe trajectory and desired trajectory in Example 1

Example 2: Consider the following desired path for the probe [38]

$$x_{des} = t$$
$$y_{des} = \frac{a}{2}\left(1 - \cos\left(\frac{\pi t}{l}\right)\right), \quad a = 20, l = 30 \tag{48}$$

Suppose that the probe is subjected to uncertainty similar to the previous example. The difference is that there is no information on the upper bound of this uncertainty. So, the robust-adaptive controllers in Theorems 4-6 are used for this example.

Consider the controller parameters as follow (the parameters are same for all of controllers)

$$\Lambda = 5 ، r = 3 ، \rho = 2 ، K = 3 \tag{49}$$

Considering the probe parameters as in (47), the simulation results have shown in Fig. 3, Fig. 4 and Fig. 5with initial condition$[x_0, y_0]^T = [1, -2]^T$.
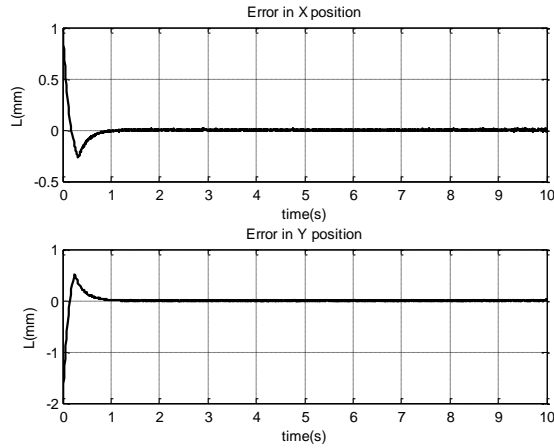

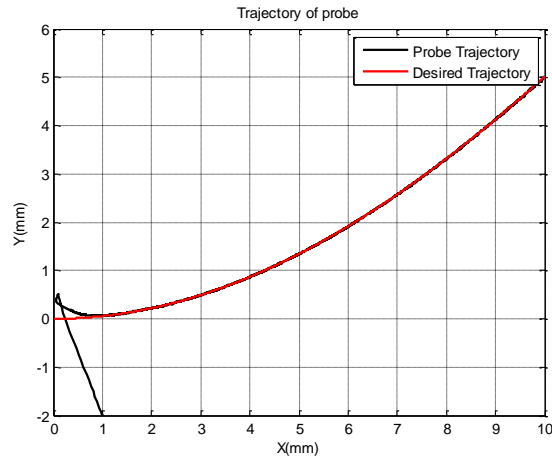Fig. 4 tracking errors in the direction of x and y in Example 2

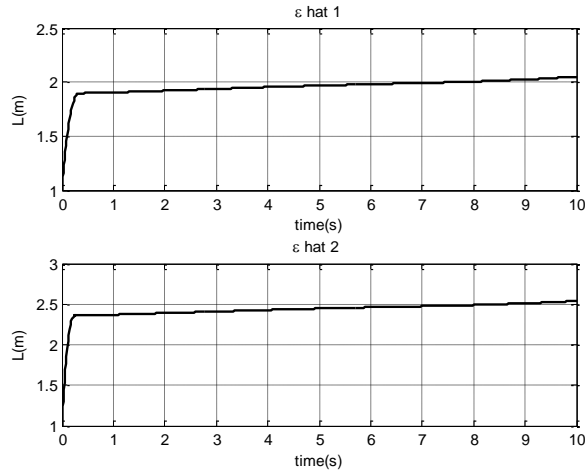Fig. 5 Probe trajectory and desired trajectory in Example 2

Fig. 6 Estimated parameters $\bar{\varepsilon}_1$ and $\bar{\varepsilon}_2$ in Example 2

Fig. 3 shows the trajectory errors that both go to zero. The trajectory of probe and desired trajectory both have been shown in Fig. 4. It is shown in this figure that the probe tracks the desired trajectory well. On the other hand, the estimations of the upper bound of disturbances have been shown in Fig. 5. This figure confirms that these estimations both are bounded.

5. Conclusions

The trajectory tracking problem of bio-inspired flexible probesin the presence of uncertainty and disturbance was dealt with. First, a robust sliding mode controller is established to deal with the uncertainties and output disturbances with this assumption that the upper band of uncertainty in the system is known. Then, an adaptive rule has been designed to estimate the upper bound of the uncertainty and disturbance and the sliding mode controller has been extended so that even if there is no information on the uncertainty, the system is still stable and the probe continues to tracks the desired trajectory. Simulation results demonstrated the effectiveness of the proposed method.

References

[1] N. Abolhassani, R. Patel, M. Moallem, "*Needle insertion into soft tissue*", e: A survey, Medical Engineering & Physics 29, (2007) 413–431.
[2] B. Davies, "*Medical robotics a bright future*", The Lancet 368 (2006) S53–S54.
[3] G. Dogangil, B. L. Davies, F. Rodriguez Baena, "*A review of medical robotics for minimally invasive soft tissue surgery*", Proceedings of the Institution of Mechanical, (2008)
[4] G. Fichtinger, T. DeWeese, A. Patriciu et. al., "*System for robotically assisted prostate biopsy and therapy with intraoperative CT guidance*", Acad Radiol, 9(1), (2004), pp. 60–74.
[5] R. Alterovitz, J. Pouliot, R. Taschereau, I. Hsu, K. Goldberg, "*Simulating needle insertion and radioactive seed implantation for prostate brachytherapy*", Stud. in Health Tech. and Informat., (2003), pp. 19– 25.
[6] N. Abolhassani, R. Patel, M. Moallem, "*Needle insertion into soft tissue: A survey*", Med. Eng. and Phys., 29(4), (2009), pp. 413–431.

[7] R. Webster, J. Kim, N. Cowan, G. Chirikjian, A. Okamura, "*Nonholonomic modeling of needle steering*", The Intl. J. of Rob. Res, 25(5-6), (2006), p. 509.

[8] S. Misra, K. Reed, A. Douglas, K. Ramesh, A. Okamura, "*Needletissue interaction forces for bevel-tip steerable needles*", in Proc. IEEE Int. Conf. on Biomed. Rob. and Biomechat., (2008), pp. 224–231.

[9] S. P. DiMaio S. E. Salcudean, "*Needle insertion modeling and simulation*", IEEE Trans. on Rob. and Auto., 19(5),(2005), pp. 864– 875.

[10] C. Duriez, C. Gu´ebert, M. Marchal, S. Cotin, L. Grisoni, "*Interactive simulation of flexible needle insertions based on constraint models*", in Proc. of MICCAI, (2009), pp. 291–299.

[11] R. Alterovitz, K. Goldberg, A. Okamura, "*Planning for steerable bevel-tip needle insertion through 2d soft tissue with obstacles*", in Proc. of ICRA, (2007), pp. 1640–1645.

[12] S. P. DiMaio, S. E. Salcudean, "*Needle steering and model-based trajectory planning*", MICCAI, (2006), pp. 33–40.

[13] V. Duindam, R. Alterovitz, S. Sastry, K. Goldberg, "*Screw-based motion planning for bevel-tip flexible needles in 3d environments with obstacles*", ICRA, (2009), pp. 2483–2488.

[14] D. Glozman, M. Shoham, "*Flexible needle steering and optimal trajectory planning for percutaneous therapies*", MICCAI, (2004), pp. 137–144.

[15] L. Frasson, S.Y. Ko, A. Turner, T. Parittotokkaporn, J.F. Vincent, F. Rodriguez y Baena, STING: "*a soft-tissue intervention and neurosurgical guide to access deep brain lesions through curved trajectories*", Proceedings of the Institution of Mechanical Engineers-Part H: Journal of Engineering in Medicine 224 (2010), pp. 775–788.

[16] S.Y. Ko, L. Frasson, B.L. Davies, F. Rodriguez y Baena, "*Software & hardware integration of a biomimetic flexible probe within the ROBOCAST neurosurgical robotic suite*", Hamlyn Symposium on Medical Robotics, London, UK, (2010).

[17] G. Fichtinger, T. DeWeese, and A. Patriciu et. al., "*System forrobotically assisted prostate biopsy and therapy with intraoperativeCT guidance*", Acad Radiol, vol. 9, no. 1 (2002), pp. 60–74.

[18] N. Abolhassani, R. Patel, M. Moallem, "*Needle insertion into softtissue: A survey*", Med. Eng. and Phys., vol. 29, no. 4, (2007), pp. 413–431.

[19] D. Glozman M. Shoham, "*Flexible needle steering and optimal trajectory planning for percutaneous therapies*", in Proc. of MICCAI, (2004), pp. 137–144.

[20] N. Abolhassani, R. Patel, F. Ayazi, "*Minimization of needle deflection in robot-assisted percutaneous therapy*", Int. J. of Med.Robot. and Comp. Assis. Surg., vol. 3, no. 2, (2007) pp. 140–148.

[21] S. Misra, K. Reed, A. Douglas, K. Ramesh, A. Okamura, "*Needletissue interaction forces for bevel-tip steerable needles*", in Proc. IEEE Int. Conf. on Biomed. Rob. and Biomechat., (2008) , pp. 224–231.

[22] S. P. DiMaio, S. E. Salcudean, "*Needle insertion modeling and simulation*", IEEE Trans. on Rob. and Auto., vol. 19, no. 5, (2003) pp. 864-875.

[23] C. Duriez, C. Guebert, M. Marchal, S. Cotin, L. Grisoni, "*Interactive simulation of flexible needle insertions based on constraintmodels*", in Proc. of MICCAI, (2009), pp. 291–299.

[24] R. Alterovitz, K. Goldberg, A. Okamura, "*Planning for steerable bevel-tip needle insertion through 2d soft tissue with obstacles*", inProc. of ICRA, (2005), pp. 1640–1645.

[25] S. P. DiMaio, S. E. Salcudean, "*Needle steering and model-based trajectory planning*", in Proc. of MICCAI, (2003), pp. 33–40.

[26] V. Duindam, R. Alterovitz, S. Sastry, K. Goldberg, "*Screw-based motion planning for bevel-tip flexible needles in 3d environments with obstacles*", Proc. of ICRA, (2008), pp. 2483–2488.

[27] S.Y. Ko, B.L. Davies, F. Rodriguez y Baena, "*Two-dimensional needle steering with a ''programmable bevel'' inspired by nature: modeling preliminaries*", IEEE/RSJ International Conference on Intelligent Robots and Systems Taipei, Taiwan, (2010), pp. 2319–2324.

[28] S.Y. Ko, L. Frasson, F. Rodriguez y Baena, "*Closed-loop planar motion control of a steerable probe with a ''programmable bevel'' inspired by nature*", IEEE Transactions on Robotics 27, (2011), pp. 970–983.

[29] R. J. Webster III, J. S. Kim, N. J. Cowan, G. S. Chirikjian, A. M. Okamura, "*Nonholonomic Modeling of Needle Steering*", The International Journal of Robotics Research, 25, (2007), pp. 509-525.

[30] R. Alterovitz, M. Branicky, K. Goldberg, "*Motion Planning Under Uncertainty for Image-guided Medical Needle Steering*", The International Journal of Robotics Research, 27, (2009), pp. 1361-1374.

[31] T. R. Wedlick A. M. Okamura, "*Characterization of pre-curved needles for steering in tissue*", in Proc. Annu. Int. Conf. IEEE Eng. Med. Biol.Soc., Sep. (2009), pp. 1200–1203.

[32] P. J. Swaney, J. Burgner, H. B. Gilbert, R. J. Webster, III, "*A flexure based steerable needle: High curvature with reduced tissue damage*", IEEE Trans. Biomed. Eng., vol. 60, no. 4, (2013) pp. 906–909, Apr.

[33] S. Okazawa, R. Ebrahimi, J. Chuang, S. E. Salcudean, R. Rohling, "*Hand-held steerable needle device*", IEEE/ASME Trans. Mechatronics,vol. 10, no. 3, (2005) pp. 285–296, Jun.

[34] S. Y. Ko, L. Frasson, F. R. y Baena, "*Closed-loop planar motion control of a steerable probe with a programmable bevel inspired by nature*", IEEE Trans. Robot., vol. 27, no. 5, (2011), pp. 970–983, Oct.

[35] K. B. Reed, A. M. Okamura, N. J. Cowan, "*Modeling and Control of Needles with Torsional Friction*", IEEE Transactions on Biomedical Engineering, 56, (2009) pp. 2905-2916.

[36] D. Glozman, M. Shoham, "*Flexible Needle Steering and Optimal Trajectory Planning for Percutaneous Therapies*", Lecture Notes in Computer Science, 3217, (2005), pp. 137-144, 2004.

[37] D. Glozman and M. Shoham, "*Image-Guided Robotic Flexible Needle Steering*", IEEE transactions on robotics, 23, (2008), pp. 459-467.

[38] S. Young Ko and F. Rodriguez y Baena, "*Trajectory following for a flexible probe with state/input constraints: An approach based on model predictive control*", Robotics and Autonomous Systems, 60, (2012), pp. 509–521.

[39] D. S. Minhas, J. A. Engh, M. M. Fenske, C. N. Riviere, "*Modeling of Needle Steering via Duty-Cycled Spinning*", in the 29th Annual International Conference of the IEEE EMBS, Lyon, France, (2007), pp. 2756-2759.

[40] D. Minhas, J. A. Engh, C. N. Riviere, "*Testing of Neurosurgical Needle Steering via Duty-Cycled Spinning in Brain Tissue in Vitro*", in IEEE EMBS, Minneapolis, Minnesota, USA, (2009), pp. 258-261.

[41] N. A. Wood, K. Shahrour, M. C. Ost, C. N. Riviere, "*Needle Steering System using Duty-Cycled Rotation for Percutaneous Kidney Access*", in International Conference of the IEEE EMBS, Buenos Aires, Argentina, (2010), pp. 5432-5435.

[42] D. Glozman, M. Shoham, "*Image-Guided Robotic Flexible Needle Steering*", IEEE Transactions on Robotics, vol. 23, (2007), pp. 459-467.